JOURNAL OF MATERIALS SCIENCE 28 (1993) 1781–1787

Dissolution of willemite polycrystals: effects of pH, temperature and TiO_2 solid solution

H. Y. CHANG, C. C. LIN, P. SHEN, A. C. SU
Institute of Materials Science and Engineering, National Sun Yat-Sen University, Kaohsiung, Taiwan

C. C. LEE
Department of Materials and Mineral Resources Engineering, National Taipei Institute of Technology, Taiwan

Dissolution (in terms of weight loss) experiments on willemite in the form of sintered polycrystals (TiO_2-dissolved or TiO_2-free) were conducted over a wide solution pH range (pH 1–13) at 25 and 50 °C, respectively, or over the temperature range 25–90 °C at pH 1. Dissolution follows a linear kinetics in acidic or basic solutions; the apparent activation energy of acid dissolution (pH 1) is 19 and 16 kJ mol^{-1}, respectively, for the TiO_2-free and the TiO_2-dissolved willemite. The pH dependence of the dissolution behaviour resembles that of zinc oxide rather than silica. Willemite polycrystals dissolve via parabolic-like kinetics in the intermediate pH range, which may be attributed to the formation of a passive film or to the possible polishing effect. TiO_2 solid solution facilitates acid but suppresses base dissolution of willemite, but grain boundary dissolution also contributes significantly in the basic region.

1. Introduction

The chemical durability of glass has been extensively studied (see [1] and references cited therein). The dissolution kinetics of silicate glasses, e.g. $(Li,Na,K)_2O$–SiO_2 [2], $(Na,K)_2O$–Ga_2O_3–SiO_2 [3], ZnO–Al_2O_3–SiO_2 [4] and systems with other compositions [5–7], have been studied. In the initial stage of dissolution in a low to medium pH range the time dependence of the dissolution rate indicates the occurrence of a de-alkali reaction [5–7]. This reaction is characterized by a linear dependence of weight loss on time and is typically diffusion-controlled [5–7]. Subsequent to this first stage, an interface-controlled reaction due to the formation of a silica-rich protective layer took place [5–7]. Phase separation of some boric oxide-bearing glasses is known to improve the chemical durability [8]. Devitrification also affects the dissolution resistance of silicate glass, e.g. crystallization from the glass based on ZnO–Al_2O_3–SiO_2, is known to decrease the acid resistivity [4].

Chemical weathering of rock-forming minerals has been of interest to geochemists. Surface processes rather than transport processes are the rate-controlling steps in the dissolution of most slightly soluble minerals (see [9] and references cited therein). For example, dissolution of silicates of various crystal structures such as feldspar (framework silicate) [10], pyroxene and amphibole (single-chain and double-chain silicates, respectively) [11–13], and olivine (orthosilicate) [13] follow a linear kinetics controlled by surface chemical reactions. Dissolution studies of nepheline (framework silicate) [14] and amorphous zircon [15] have indicated that precipitation of new phases from solution may lower the dissolution rate [14, 15]. With increasing pH, a decrease in the dissolution rate in the acid region and then an increase in the dissolution rate in the basic region are typically observed for silicate minerals (see [16] and references cited therein); this type of rate data has been interpreted as the result of surface speciation in the dissolution of minerals [17]. In general, congruent dissolution (e.g. olivine [13, 18] and nepheline [14]) or incongruent dissolution (e.g. chain silicates [12, 18] and feldspar [18]) may occur at a certain stage of dissolution, and the constraints are provided by adsorption equilibria, surface ion-exchange reactions and the pH dependence of the steady-state rates of surface detachment [18]. A preferential release of cations from specified structural sites (e.g. the M_2 sites of pyroxene) may explain the incongruent reaction at the mineral surface [12].

Willemite (α–Zn_2SiO_4) which has phenacite structure with its SiO_4 polymerized to other tetrahedra by sharing corners with ZnO_4 (see [19, 20] and references cited in [20]) is commonly found in zinc-ore deposit, crystalline glaze [21] and glass ceramics [22]. Willemite was chosen for the present dissolution kinetics study because all of its cations are of tetrahedral coordination, which is unique to other silicates already studied for dissolution kinetics [9–18]. The temperature and pH dependence of willemite dissolution may also shed light on the dissolution resistance of the

willemite-bearing glaze and glass ceramics. It is commonly accepted that the addition of TiO_2 facilitates nucleation and hence devitrification of glass ceramics [8]. TiO_2 addition also reduces the activation energy of willemite formation from constituent oxides [23]. Also reported here is the effect of solid solution of TiO_2 in willemite (2.5 mol % at 1500 °C [23]) on its dissolution resistance in acidic or basic solutions.

2. Experimental procedure

2.1. Starting materials

Stoichiometric ZS powder ($ZnO:SiO_2 = 2:1$ in molar ratio) and ZST powder (obtained by the introduction of 2 mol % TiO_2 to ZS) were prepared by stirring powder mixtures of ZnO [Cerac, USA; 99.9% purity with trace impurities (in p.p.m.): 35Al, 5Li, 5Ca, 5Cr, 5Na, 5Fe, 5Zr, 3K, 2Mn, 2Ti, 1Cu, 1Mg and 1B], SiO_2 [Cerac, USA; 99.9% purity with trace impurities (in p.p.m.): 400Al, 200Ca, 300Fe and 80Mg] and TiO_2 [Cerac, USA; 99.9% purity with trace impurities (in p.p.m.): 10Al, 10Sn and 10Si) in deionized water, dried at 200 °C, then calcined at 500 °C for 4 h. Powders weighing approximately 300 mg were die-pressed at 50 MPa to discs 10 mm in diameter and only about 0.5 mm thick so that the weight loss during dissolution was mainly from the parallel circular faces. The ZS and ZST samples were then enveloped in platinum foil, placed in an alumina crucible, and fired at 1430 °C for 4 h followed by furnace-cooling.

The sintered ZS and ZST specimens showed negligible weight loss. The complete reaction of constituent oxides to form willemite was confirmed by X-ray diffraction (XRD). In comparison with the ZS sample, larger X-ray *d*-spacings for ZST were indicated by the XRD results. This is attributed to the dissolution of TiO_2 in willemite of the specimen ZST. Scanning electron microscopy (SEM; JSM35CF, operating at 25 kV) indicated that the willemite grains in ZS and ZST specimens were, respectively, approximately 10 and 100 μm in size and the grain morphology was characteristic of that sintered beyond the intermediate stage.

2.2. Analytical methods

Fired pellets, either unpolished or polished with diamond paste (6 μm particle size), were ultrasonically cleaned, rinsed with distilled water and then subjected to static dissolution experiments in a plastic beaker. The ingredients of the buffer solutions for dissolution experiments are given in Table I. The weight loss of each sample was measured to 0.1 mg and the average of five independent measurements were recorded. SEM was used to take secondary-electron images (SEI) of the sample surface before and after the dissolution experiments. XRD was used when necessary to identify the products.

TABLE I Constituents of buffer solutions at specified pH values

pH	Buffer solution
1	HCl–glycine
4	HCl–glycine
7	KH_2PO_4–Na_2HPO_4
7	KH_2PO_4–Na_2HPO_4–NaCl(0.3 M)
10	NH_4OH–NH_4Cl
13	KCl–NaOH

3. Results

3.1. Temperature and pH dependence

In the temperature range 25–90 °C (Fig. 1a–d) the isothermal dissolution of polycrystalline willemite in a buffer solution at pH 1 showed a higher dissolution rate for the ZST than for the ZS specimen. The dissolution rates of both ZST and ZS specimens increased with temperature, with the former slightly less sensitive to temperature, so that the difference in weight loss became less apparent at higher temperature (Fig. 1). Values of the apparent activation energy as estimated by the corresponding Arrhenius plots (Fig. 2) were 19.2 ± 0.9 and 15.6 ± 0.9 kJ mol^{-1}, respectively, for ZS and ZST at pH 1.

Isothermal (50 °C) and isochronical (3.5 h) dissolution experiments were conducted to study the pH dependence of the dissolution rate (Fig. 3). A large decrease in the dissolution rate with increasing pH in the acid region and a slight increase in the dissolution rate with pH in the basic region were observed for both ZS and ZST specimens. Compared with the ZS specimen, the ZST specimen showed a higher dissolution rate in the acid region but a lower dissolution rate in the basic region.

3.2. Dissolution kinetics

Isothermal (25 °C) dissolution experiments of ZS at pH 1, 4, 7, 10 and 13 were conducted to study the time dependence of the weight loss. At pH 1 a linear dissolution kinetics was observed (Fig. 4a). At pH 4 (Fig. 4b) and pH 7 (Fig. 4c) parabolic-like kinetics became significant, but deviation was observed after prolonged dissolution. Fig. 5 is the parabolic plot for the first four data points of Fig. 4c, showing that the dissolution follows a $t^{1/2}$ dependence in the early stage. A linear dissolution kinetics was observed again at pH 10 (Fig. 4d) and pH 13 (Fig. 4e). In contrast to that observed in NaCl-free solution at pH 7 (Fig. 4c), linear rather than parabolic-like kinetics was obeyed in the presence of NaCl (Fig. 4f).

3.3. Surface roughness and crystal orientation dependence

Isothermal (25 °C) dissolution of the polished ZS samples at pH 1, 4, 7, 10 or 13 indicated that the dissolution mechanism itself is not extremely sensitive to polishing treatment (Fig. 6a–e). However, higher weight losses were consistently observed for polished samples. This is in agreement with the preferential dissolution along scratches on the polished surface of a willemite single crystal [24]. Dissolution along the grain boundary was observed upon SEM for both ZS and ZST specimens, especially in basic solutions, in

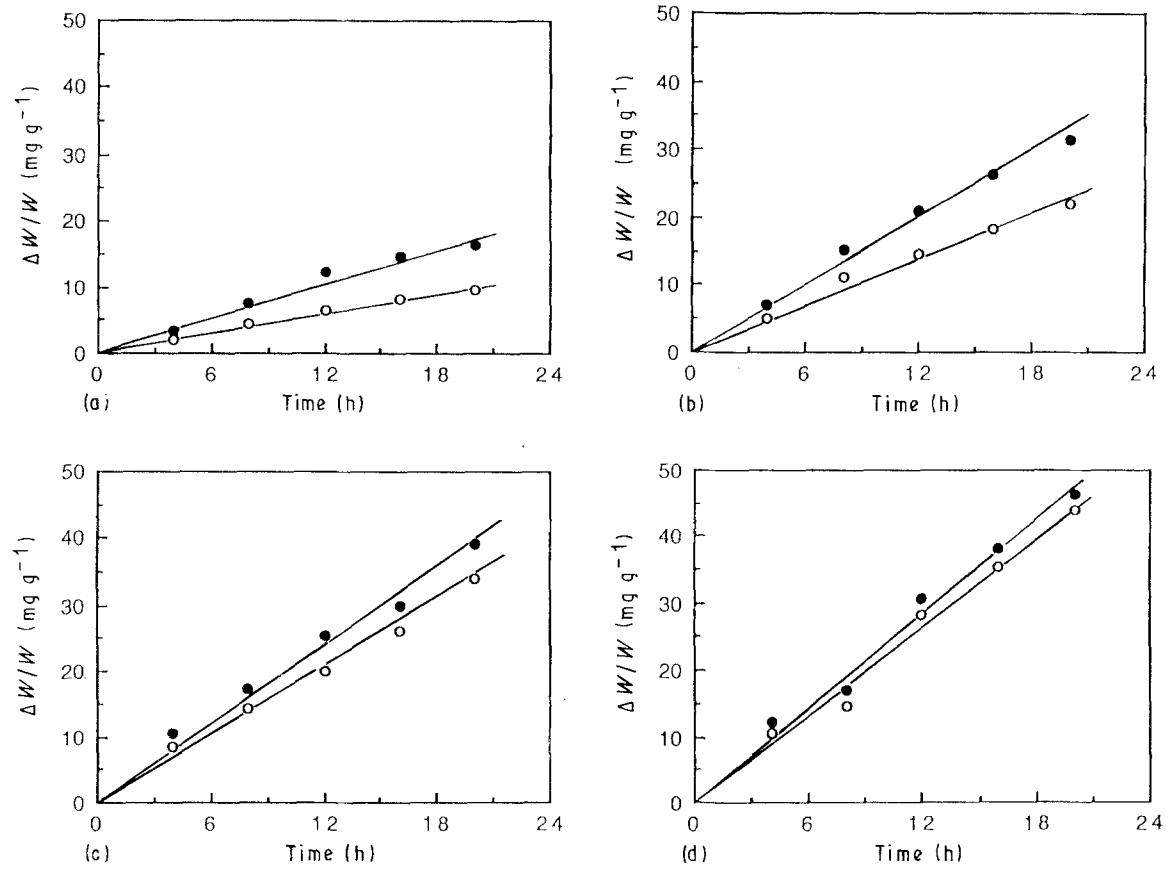

Figure 1 Weight loss of (○) ZS specimen and (●) ZST specimen at pH 1 at (a) 25 °C, (b) 50 °C, (c) 75 °C and (d) 90 °C.

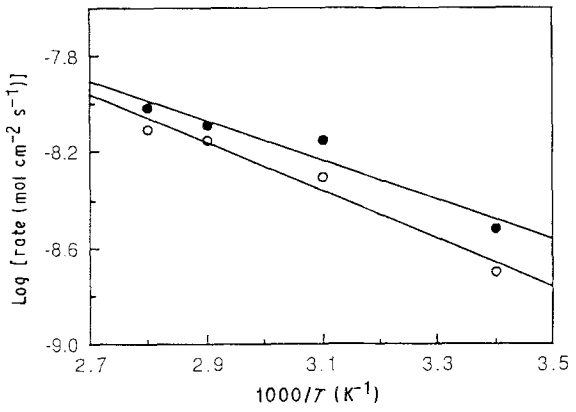

Figure 2 Plot of log [dissolution rate (mol $Zn_2SiO_4 cm^{-2} s^{-1}$)] versus inverse temperature to determine the activation energy at pH 1: (○) ZS and (●) ZST.

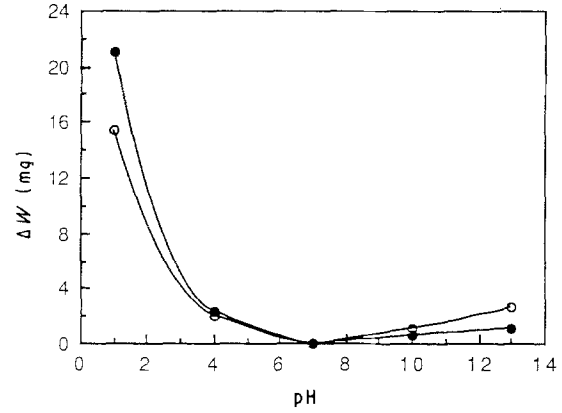

Figure 3 Isochronical (3.5 h) and isothermal (50 °C) weight loss of (○) ZS specimens and (●) ZST specimens at various pH values.

which intragranular dissolution is slow. Etching pits and hillocks could be clearly observed in some of the larger grains of the ZST specimen. In the case of ZS, no etching pits or orientation effect could be identified due to the smaller grain size. The extensive formation of etching pits in some but not all grains indicated that dissolution depends on the crystal orientation. This is consistent with a separate observation of preferential dissolution along the *c*-axis in a willemite single crystal [24].

4. Discussion

4.1. Reaction-controlled dissolution

A number of silicate minerals (e.g. feldspars, pyroxenes and amphiboles) dissolve via linear rather than parabolic kinetics over a wide pH range; the dissolution rate is controlled by surface chemical reaction forming angular rather than round etch pits [9]. Although some cation depletion (relative to silicon), may occur (e.g. in pyroxenes), the depleted surface layer (if it exists) is generally too thin to be described as a diffusion barrier [9]. In acid and basic solutions the present willemite samples also dissolved via linear kinetics; the dissolution appeared to be controlled by surface chemical reaction, as indicated by the characteristic etch pits. The parabolic kinetics of willemite at pH 7 and 4 could be due to the deposition of a passive film, but is also likely to be an artifact of surface irregularities from polishing as discussed in Section 4.2.

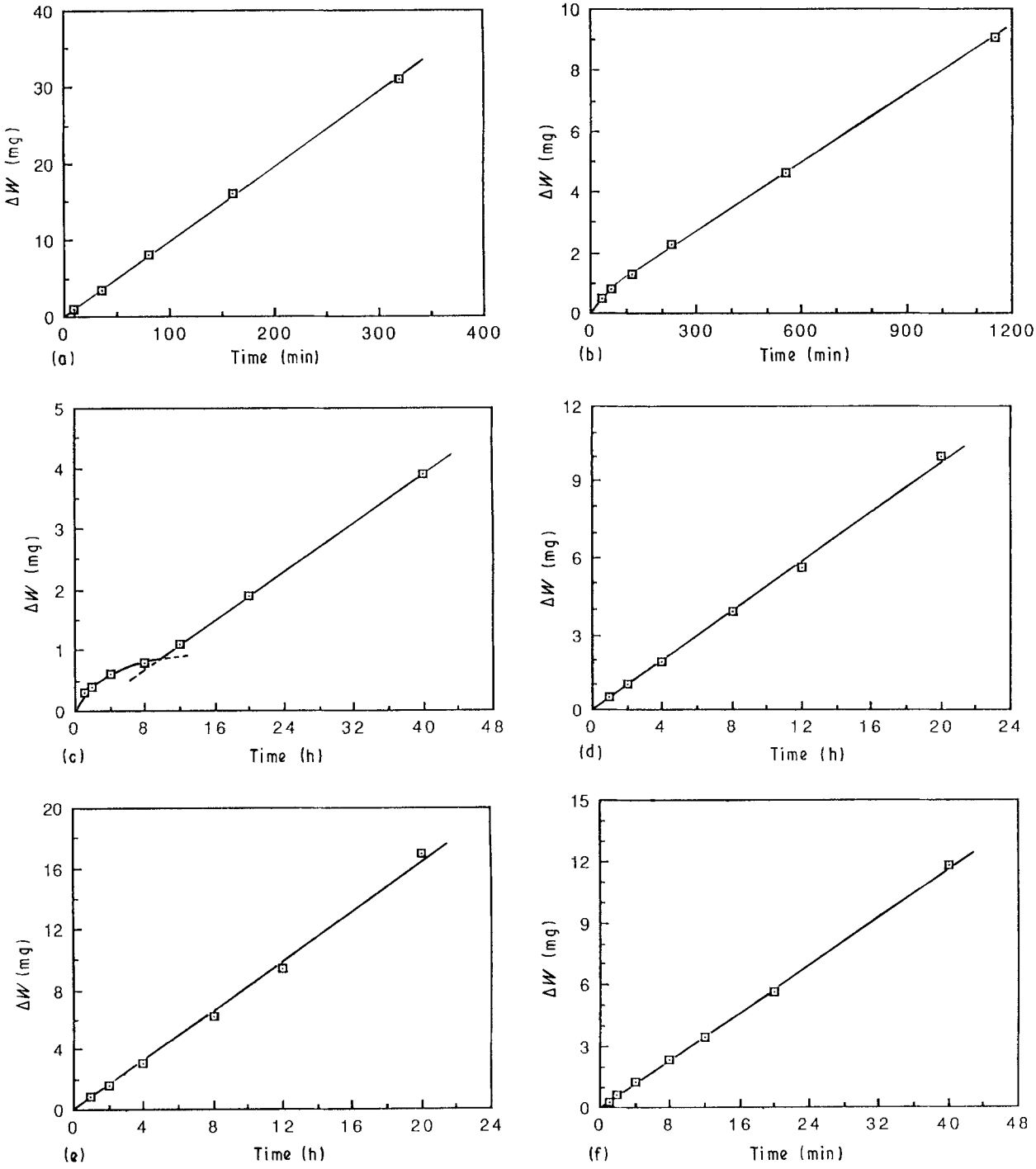

Figure 4 Isothermal (25 °C) dissolution kinetics of ZS specimens at (a) pH 1, (b) pH 4, (c) pH 7, (d) pH 10, (e) pH 13 and (f) pH 7 with added NaCl in solution.

4.2. Interpretation of pH and NaCl dependence

4.2.1. pH dependence

The pH dependence of the steady-state dissolution rates of silicates in the literature is explained by the detachment rate of their oxide components through surface protonation–deprotonation reactions [25]. In the high pH range, where silicon surface sites are presumably deprotonated and therefore negatively charged, detachment of silicon is expected to control the overall silicate dissolution rate. At low pH, where the zero point of charge (ZPC is approximately 2 for various kinds of SiO_2 [26]) of SiO_2 is approached, the surface charge is dominated by the other oxide components, detachment of the non-silicon structure-forming oxides should control the dissolution rate of multi-oxide silicates [25].

Willemite (either TiO_2-bearing or TiO_2-free) is quite base-resistant but dissolves extensively in acid solutions. This behaviour is similar to that of metallic zinc [27], but the opposite of the dissolution of silica from quartz [28], indicating that the weight loss of the ZS and ZST specimens is probably controlled by extraction of the zinc ion rather than the silica anion, especially in the low-to-medium pH region. This is consistent with the estimated isoelectric point (IEP) of willemite (pH $\approx$ 7 according to the weighted average of the constituent oxides [29]), indicating that the willemite surface is positively charged for pH < 7. The IEP of SiO_2 (quartz or sol–gel) and ZnO (anhydrous

or hydrous) are about 2 and 9–10, respectively [26], suggesting also that the dissolution of willemite is controlled by leaching of ZnO in the acidic region, whereas the leaching of silica probably determines the dissolution (although a low rate was observed) of willemite in the basic region.

It has been suggested that the "parabolic kinetics" obtained for some feldspar dissolution studies is the result of the various rates of dissolution of particles produced during grinding [9, 10]. Initial dissolution should therefore be faster due to preferential dissolution of the fine particles, and deceleration with time should occur as the small particles are consumed. The apparent parabolic-like kinetics in the early stage of dissolution (and the subsequent linear dissolution behaviour) for the present willemite specimens at pH 7 or 4 may therefore be attributed (at least in part) to a grinding artefact. However, the possibility that willemite may form $Zn(OH)_2$ (as in the case of metallic zinc [30]) or a $ZnHPO_4$ surface layer which serves as a diffusion barrier and results in the parabolic dissolution rate in the nearly neutral environment cannot be completely excluded.

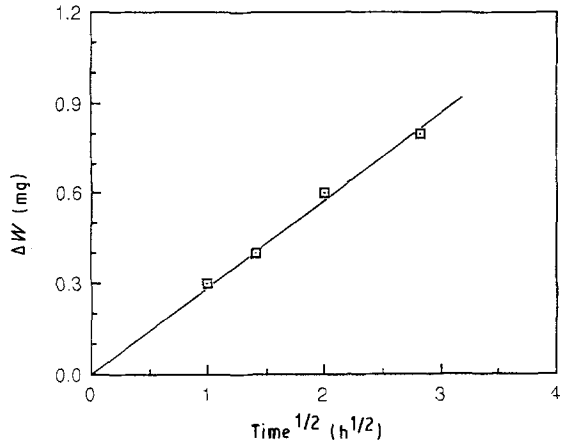

Figure 5 Parabolic plot of the short-period dissolution of Fig. 4c.

4.2.2. NaCl dependence

Foreign ions affect the activation energies for the surface reaction (ΔG_r) and the subsequent detachment (ΔG_d), and hence affect the total dissolution rate [31]. Since the complex formation from ligand occurs in solution as well on the solid surface [29], the stability constant or solubility of the appropriate complexes in solution may be used to infer the NaCl dependence of willemite dissolution. The ZS specimens showed comparatively poor dissolution resistance in the NaCl-added solution (Fig. 4f), indicating that Cl^- probably

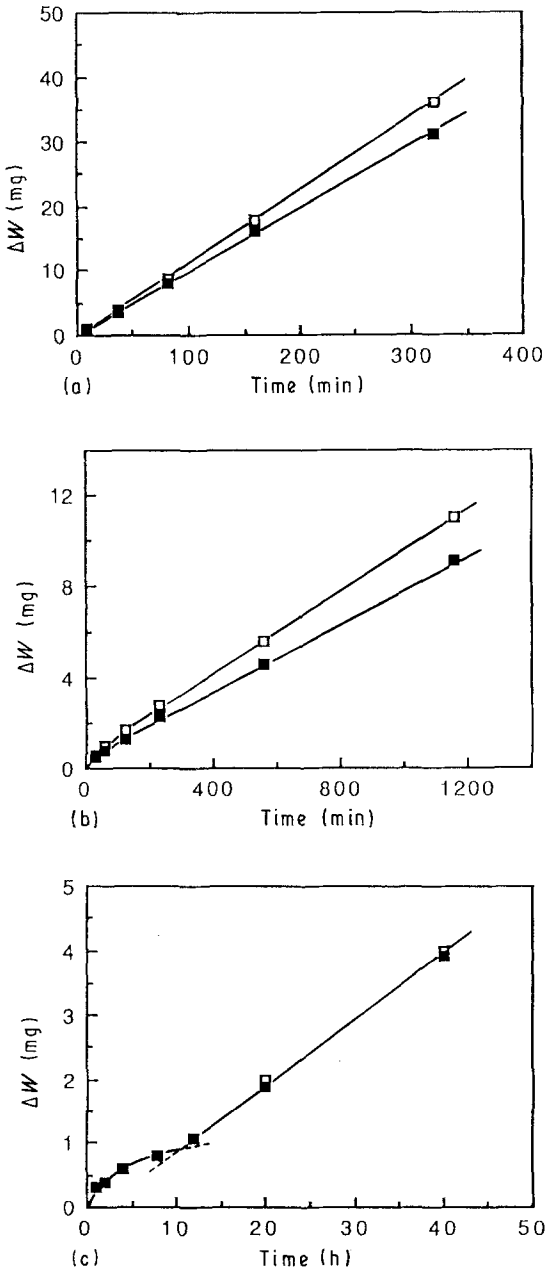

Figure 6 Weight loss of (○, □) polished and (●, ■) as-sintered ZS specimens at 25 °C and (a) pH 1, (b) pH 4, (c) pH 7, (d) pH 10 and (e) pH 13.

affects the dissolution behaviour. Ligands, e.g. phosphate and chloride in acid solution, have been known to accelerate the dissolution of oxides of single component [32]. This consideration is extended to the dissolution of oxides of multiple components (viz. willemite) in the following.

In view of the IEPs of the constituent oxides, it is likely that the detachment of zinc ion cannot be neglected for the willemite dissolution at medium pH values. One possible explanation is that a barrier layer of $Zn(OH)_2$ and/or $ZnHPO_4$, the overall stability constant of which are about 10^{18} [33] and 10^{14} (see [34] and references cited therein), respectively may form in the absence of NaCl. The passive layer could be deposited from solution or formed directly on the surface. In the presence of Cl^- the formation of a passive film could be interrupted by a series of reactions involving zinc chlorides whose overall stability constants ($< 10^{-2}$) are much lower than that of hydroxide or phosphate. It is therefore likely that Cl^- catalyses the overall reaction by competing with the surface adsorption and subsequent detachment through chlorides. However, other possibilities do exist. For example, the adsorption of Cl^- may increase the H^+ activity, and hence increase the dissolution rate because the IEP shifts to lower pH whereas the zero point of charge (pH_{zpc}) moves to higher pH when surface adsorption of a foreign anion occurs [29]. Further study is required to clarify the real effect of Cl^- on the dissolution of willemite.

4.3. Relative dissolution rates of silicates

Willemite exhibits a much higher dissolution rate (about two to eight orders of magnitude higher) than common rock-forming silicates at room temperature and pH 1 (e.g. 10^{-8} mol cm^{-2} s^{-1} for willemite (Table II) compared with 10^{-12} mol cm^{-2} s^{-1} for olivine) [25]. This could be attributed to the site-energy dependence of dissolution or other factors as discussed below.

In general the dissolution rate of common rock-forming silicates increase with decreasing mean electrostatic oxygen site potential, i.e. increasing silica release rate (see [25] and references cited therein). Recently a general rate law for the acid- and ligand-promoted dissolution of minerals has been proposed [35]. According to Wieland *et al.* [35] the dissolution rate (at pH around 5) for many minerals, especially oxides, shows a tendency to increase with decreasing apparent activation energy. This supports the hypothesis [25] that the site energy (Madelung energy) of the most stable lattice constituents (generally a metal cation at a surface site) or the ion-formation energy of the solid are suitable free-energy parameters to be correlated with the dissolution rate. It should be noted that the dissolution rates of silicates generally have a higher deviation than that predicted by the activation energy (or site energy) [35]. This indicates that other energy terms (e.g. the surface or interfacial energy and strain energy, either at a dislocation core or at scratches caused by polishing) affect the dissolution kinetics of silicates. Willemite has higher dissolution rate than the common silicates in the acidic region. This could be attributed in part to the grain boundary effect, or could be due to the unique phenacite structure of willemite, which determines the types of dislocations or other defects for short-circuit dissolution, although the types of defects and their physical mechanism of dissolution are by no means clear.

TABLE II Temperature dependence of dissolution rate (mol cm^{-2} s^{-1}) at pH 1

T (°C)	ZS	ZST	log (dissolution rate)	
			ZS	ZST
25	2×10^{-9}	3×10^{-9}	− 8.7	− 8.5
50	5×10^{-9}	7×10^{-9}	− 8.3	− 8.2
75	7×10^{-9}	8.2×10^{-9}	− 8.2	− 8.1
90	7.8×10^{-9}	9.6×10^{-9}	− 8.1	− 8.0

4.4. Effect of TiO_2 solid solution on dissolution of willemite

Within the present temperature range the ZST specimens showed a higher dissolution rate than the ZS specimens in the low-pH region. The trend was exactly reversed in the high-pH region. The solubility of TiO_2 in willemite is 2.5 mol % at 1500 °C and Ti^{4+} probably occupies the tetrahedral site in order to maintain a polymerized ZnO_4–SiO_4–ZnO_4 chain [23]. Therefore, the difference in the dissolution rates of the ZS and ZST specimens can be attributed to the solid solution of TiO_2 in the willemite lattice, which affects the oxygen site potential as described in the following. First, substitution of Ti^{4+} for Si^{4+} (or less probably Zn^{2+} if a charge-compensating defect is available) in willemite may introduce distortion of the lattice in view of the differences in the ionic radii in four-co-ordination (0.042, 0.026 and 0.060 nm for Ti^{4+}, Si^{4+} and Zn^{2+}, respectively [36]). Therefore, in the vicinity of the incorporated Ti^{4+} ion the oxygen site potential is lowered, which generally results in a higher dissolution rate [25]. The IEP of TiO_2 (rutile or anatase) is 5–6, which falls between that of SiO_2 and ZnO [26], suggesting that dissolution of the ZST specimen is controlled by the detachment of ZnO in acid and of silica in the basic region, rather than the leaching of Ti^{4+}. When silica leaching is predominant in the basic region, the incorporation of Ti^{4+} decreases the site density of silicon and hence lowers the dissolution rate.

The dissolution of willemite single crystal is much slower than that of polycrystals in the basic region [24]. The difference in dissolution rate of the ZS and ZST specimens in the basic region may therefore be attributed in part to the difference in grain size. In the acidic region the rapid dissolution of grain bulk and the effect of TiO_2 solid solution in willemite probably overshadowed the grain size effect. The grain size effect is also of minor importance at higher temperatures, where intragranular dissolution is more extensive for both ZS and ZST specimens. Previous dissolution studies of feldspars in the pH range 3–9

also indicated that the dissolution rate is surface-reaction-controlled rather than surface-area-controlled [37], with crystalline defects (e.g. the lamellae interface) being the preferred reaction sites [37, 38].

5. Conclusions

1. Willemite polycrystals dissolve via linear kinetics in highly acidic or basic solutions.

2. The pH dependence of willemite dissolution resembles that of metallic zinc, especially in the acidic region.

3. Parabolic-like dissolution of willemite polycrystals, which occurs at intermediate pH levels, could be due to artefacts of polishing or the formation of a passive film.

4. The activation energy of acid dissolution (pH 1) is 19 and 16 kJ mol^{-1} for TiO_2-free and TiO_2-dissolved willemite, respectively.

5. TiO_2 solid solution facilitates the acid but suppresses the basic dissolution of willemite, although a contribution from grain boundary dissolution is perceptible in the basic region.

6. I.E.P. of willemite is 7.4 according to experimental results [39].

7. The fact that Ti^{4+} occupies the tetrahedral site of willemite has been reported [40].

Acknowledgement

This work was supported in part by National Science Council, Taiwan, under contract NSC79-0405-E110-12.

References

1. H. RAWSON, "Glass Science and Technology", Vol. 3: "Properties and Applications of Glass" (Elsevier, Amsterdam, 1980).
2. R. W. DOUGLAS and T. M. M. EL-SHAMY, *J. Amer. Ceram. Soc.* **50** (1967) 1.
3. J. C. LAPP and J. E. SHELBY, *ibid.* **70** (1987) 271.
4. M. SHIMBO, *ibid.* **70** (1987) C101.
5. R. J. CHARLES, *J. Appl. Phys.* **29** (1958) 1549.
6. T. M. EL-SHAMY, J. LEWIS and R. W. DOUGLAS, *Glass Technol.* **13** (1972) 81.
7. R. H. DOREMUS, in "Glass Science" (Wiley, New York, 1973) p. 229.
8. P. W. McMILLAN, "Glass Ceramics", 2nd Edn (Academic Press, London, 1979) p. 90.
9. R. A. BERNER, in "Reviews in Mineralogy", Vol. 8: "Kinetics of Geochemical Processes", edited by A. C. Lasaga and R. J. Kirkpatrick (Mineralogical Society of America, Washington, DC, 1981) p. 111.
10. R. A. BERNER and G. R. HOLDREN, Jr, *Geochim. Cosmochim. Acta* **43** (1979) 1173.
11. R. A. BERNER, E. L. SJOBERG, M. A. VELBEL and M. D. KROM, *Science* **207** (1980) 1205.
12. J. SCHOTT, R. A. BERNER and E. L. SJOBERG, *Geochim. Cosmochim. Acta* **45** (1981) 2123.
13. J. SCHOTT and R. A. BERNER, *ibid.* **47** (1983) 2233.
14. M. P. TOLE, A. C. LASAGA, C. PANTANO and W. B. WHITE, *ibid.* **50** (1986) 379.
15. M. P. TOLE, *ibid.* **49** (1985) 453.
16. A. C. LASAGA, *J. Geophys. Res.* **89** (B6) (1984) 4009.
17. A. E. BLUM and A. C. LASAGA, *Nature* **331** (1988) 431.
18. W. M. MURPHY and H. C. HELGESON, *Geochim. Cosmochim. Acta* **51** (1987) 3137.
19. M. A. SIMONOV, P. A. SANDOMIRSKII, Y. K. EGOROV-TISMENKO and N. V. BELOV, *Soviet Phys. Dokl.* **22** (1977) 622.
20. J. A. SPEER and P. H. RIBBE, in "Reviews in Mineralogy", Vol. 5: "Orthosilicates", 2nd Edn, edited by P. H. Ribbe (Mineralogical Society of America, Washington, DC, 1982) p. 429.
21. F. H. NORTON, *J. Amer. Ceram. Soc.* **20** (1937) 217.
22. P. W. McMILLAN, *Phys. Chem. Glasses*, **10** (1969) 153.
23. C. C. LEE, P. SHEN and H. Y. LU, *J. Mater. Sci.* **24** (1989) 3300.
24. C. C. LIN and P. SHEN, *Geochim. Cosmochim. Acta* in press.
25. P. V. BRADY and J. V. WALTHER, *Geochim. Cosmochim. Acta* **53** (1989) 2823.
26. G. A. PARKS, *Chem. Rev.* **65** (1965) 177.
27. M. POUBAIX, in "Atlas of Electrochemical Equilibria in Aqueous Solutions" (National Association of Corrosion Engineers, Houston, Texas, 1974) p. 410.
28. K. KNAUSS and T. WOLERY, *Geochim. Cosmochim. Acta* **52** (1988) 43.
29. W. STUMM and J. J. MORGAN, in "Aquatic Chemistry: An Introduction Emphasizing Chemical Equilibria in Natural Waters" (Wiley–Interscience, New York, 1981) p. 632.
30. R. J. BRODD and V. E. LEGER, in "Encyclopedia of Electrochemistry of the Elements", Vol. 5, edited by A. J. Bard (Marcel Dekker, New York, 1976) p. 1.
31. A. C. LASAGA, in "Kinetics of Geochemical Processes", edited by A. C. Lasaga and R. J. Kirkpatrick (Mineralogical Society of America, Washington, DC, 1981) p. 1.
32. R. GRAUER and W. STUMM, *Colloid Polym. Sci.* **260** (1982) 959.
33. R. C. WEAST and D. R. LIDE (editors), in "Handbook of Chemistry and Physics" (CRC Press, Boca Raton, Florida, 1989) p. B–208.
34. J. INCZEDY, in "Analytical Applications of Complex Equilibria" (Ellis Horwood, Chichester, 1976) p. 317.
35. E. WIELAND, B. WEHRLI and W. STUMM, *Geochim. Cosmochim. Acta* **52** (1988) 1969.
36. R. D. SHANNON, *Acta Crystallog* **A32** (1976) 751.
37. G. R. HOLDREN, Jr and P. M. SPEYER, *Geochim. Coschim. Acta* **49** (1985) 675.
38. *Idem, ibid.* **51** (1987) 2311.
39. R. SPRYCHA, Colloids Surf. **5** (1982) 147.
40. P. TARTE, *Nature* **191** (1961) 1002.

Received 11 September 1991
and accepted 2 September 1992